Materials Science in Semiconductor Processing 27 (2014) 145–149

Contents lists available at ScienceDirect

Materials Science in Semiconductor Processing

journal homepage: www.elsevier.com/locate/mssp

Gaussian distribution of inhomogeneous barrier height in Au/n-Si (111) Schottky barrier diodes at low temperatures

Perihan Durmuş [a], Mert Yıldırım [b,*]

[a] Physics Department, Faculty of Sciences, Gazi University, 06500 Teknikokullar, Ankara, Turkey
[b] Physics Department, Faculty of Arts and Sciences, Düzce University, 81620 Konurap, Düzce, Turkey

ARTICLE INFO

Available online 9 July 2014

Keywords:
I–V characteristics
Inhomogeneous barrier
Gaussian distribution of barrier
Modified Richardson plot

ABSTRACT

Forward bias current–voltage (*I–V*) characteristics of Au/n-Si (111) Schottky barrier diode (SBD) were investigated in the temperature range of 80–290 K. Analysis of temperature dependent *I–V* data in terms of thermionic emission (TE) theory revealed an abnormal increase in zero-bias barrier height (Φ_{Bo}) and decrease in ideality factor (n) with increasing temperature. Such behavior of Φ_{Bo} and n was attributed to barrier inhomogeneities by assuming a Gaussian distribution (GD) of barrier height. Therefore, mean barrier height and effective Richardson constant (A^*) values were extracted from the modified Richardson plot, and extracted A^* was found close to the theoretical value for n-type Si. Hence, it has been concluded that temperature dependent *I–V* characteristics of the SBD can be successfully explained on the basis of TE theory with GD of barrier height. In addition, series resistance and energy profile of density of interface traps in the SBD were also investigated.

1. Introduction

Since their first discovery by Braun [1], metal–semiconductor (MS) structures were thoroughly investigated by many researchers since these structures constitute the basic part of many electronic devices. Nevertheless, full understanding of the electrical characteristics of these type of Schottky barrier diodes (SBDs) has not been achieved since electrical parameters of MS SBDs are highly dependent under operation conditions. As reported in various studies [2–16], performance of these kinds of structures is highly effected by its series resistance (R_s) and density of interface traps (D_{it}). These parameters are the main reasons that the electrical characteristics of an MS SBD deviate from those of an ideal MS SBD. This is probably due to the fact that a very thin oxide layer might be formed between metal and semiconductor during a fabrication process despite the efforts to prevent. Studies on these kinds of structures in the literature basically focus on thermionic emission (TE) theory and obtain electrical parameters with this assumption [2,4,7–16]. However, in the case of inhomogeneous barrier potential between metal and semiconductor, the structure's barrier potential is resembled to a barrier consisting of higher and lower patches from which current pass through. Thus, it is possible to explain it through TE theory with Gaussian distribution (GD) of barrier potential [10–15].

Over the years, researchers conducted studies on MS SBDs; among these studies the ones that consider the electrical characteristics while the operation temperature is changed come forward since the investigation of electrical characteristics only at room temperature does not provide much about the nature of the structure. Furthermore, some of practical applications of MS SBDs require these structures to operate at low or high temperatures; therefore it is a necessity to study these structures in a

* Corresponding author.
E-mail address: mertyildirim@duzce.edu.tr (M. Yıldırım).

http://dx.doi.org/10.1016/j.mssp.2014.06.047
1369-8001/

wide temperature range. Also, temperature dependent investigation of electrical characteristics gives insight into the dominant current conduction mechanism in the structure. Therefore, in the present study, Au/n-Si (111) MS SBD was fabricated and its current–voltage (I–V) measurements were held between 80 K and 290 K so that its electrical characteristics were investigated between −2 V and +2 V. Obtained results indicated inhomogeneous barrier potential; hence Au/n-Si (111) MS SBD I–V characteristics were explained by TE with GD of barrier potential.

2. Experimental details

For the fabrication of MS SBD, the substrate was chosen as n type Silicon doped with Phosphorus having donor concentration of $\sim 1.1 \times 10^{15}$ cm^{-3}, (111) surface orientation, $\sim 1\,\Omega$ cm resistivity, 3 in. diameter, and 350 μm thickness. First, the substrate, front and back contact material, and required equipment were applied to the chemical cleaning process in order to remove any contaminants and/or any previously formed oxide layer. Details of cleaning process were given elsewhere [3,4]. Afterwards, back side of the substrate was deposited Au (with purity of 99.999) layer of 200 nm through thermal evaporation system which is kept at vacuum of $\sim 10^{-6}$ Torr. For the deposited layer to exhibit ohmic feature, the substrate was annealed at 450 °C for 4 min in N_2 environment so that the Au layer is sintered. Afterwards, the substrate was taken into thermal evaporator system, to which same conditions were applied, again for deposition of front contact of 200 nm Au layer with diameter of 1 mm. Thus, Au/n-Si MS SBD is fabricated. Then a sample was prepared and mounted on the Janis vpf-475 cryostat whose temperature is controlled by the Lake Shore model 321 auto-tuning temperature controller while vacuum environment of 5×10^{-4} Torr is ensured in the cryostat for the measurements. Afterwards, I–V measurements were conducted between 80 K and 290 K using the Keithley 2400 sourcemeter which is connected to a computer through the IEEE-488 ac/dc converter card.

3. Results and discussion

As mentioned earlier, R_s causes I–V characteristics of MS SBDs to be non-ideal. This is mainly because the voltage drop due to R_s. Fig. 1 shows temperature dependent I–V plots of MS SBD and schematic representation of the SBD. It is seen that MS SBD rectifies successfully with a fair rectifying ratio (RR) for each temperature level. RR at 290 K is $\sim 2.5 \times 10^3$ while it is 10^5 at 80 K due to smaller leakage current values at lower temperatures. As seen in Fig. 1, all I–V plots have a linear region in the forward bias region up to ~1 V; all plots bend due to R_s above 1 V. Therefore, it is important to obtain R_s values before going any further. Simplest way of obtained R_s values is Ohm's law which yields R_s as dV/dI in the high forward bias region. Therefore, R_s values of MS SBD is calculated using Ohm's law. It is often that R_s values were also calculated with other techniques such as Cheungs' method in order to cross-check with Ohm's law [4,12,14,16]. For this purpose,

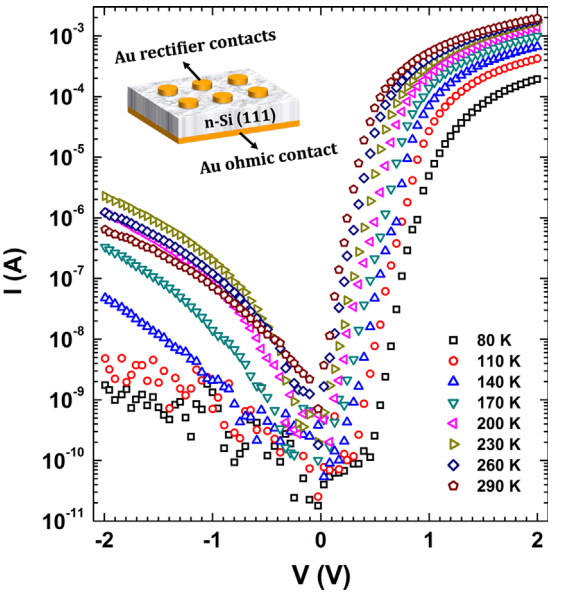

Fig. 1. I–V plots of Au/n-Si MS SBD and schematic representation of MS SBD.

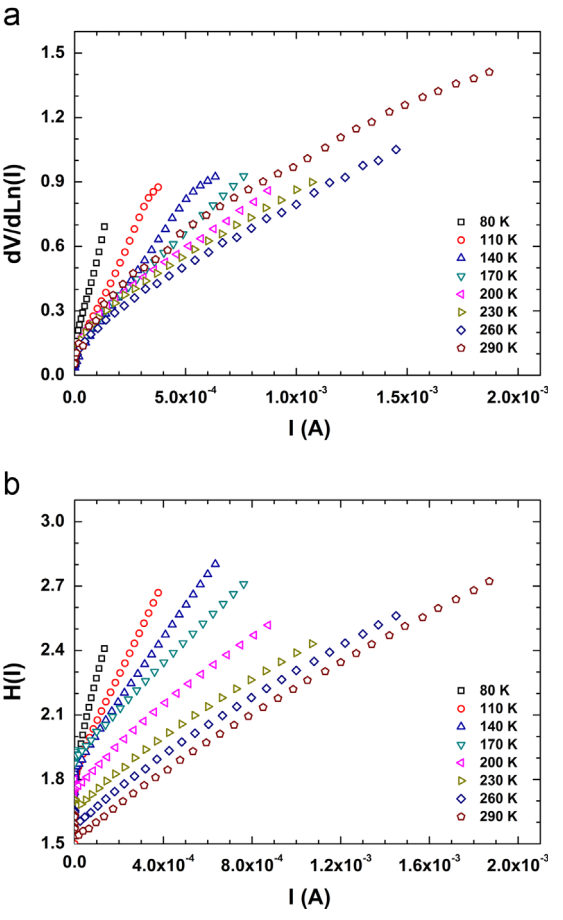

Fig. 2. (a) dV/dln(I)–I and (b) $H(I)$–I plots of Au/n-Si MS SBD.

Table 1
Temperature dependent main electrical parameters of Au/n-Si MS SBD.

T (K)	I_o (A)	n	Φ_{Bo} (eV)	R_s (kΩ)		
				R_i–V	$dV/d\ln(I)$–I	$H(I)$–I
80	3.44×10^{-14}	5.43	0.241	4.23	3.91	3.99
110	1.54×10^{-13}	4.71	0.323	2.23	2.09	2.13
140	6.62×10^{-13}	4.11	0.399	1.46	1.45	1.46
170	6.22×10^{-11}	3.77	0.424	1.05	0.99	1.02
200	1.03×10^{-10}	3.03	0.496	0.77	0.73	0.75
230	1.47×10^{-10}	2.63	0.569	0.66	0.59	0.61
260	6.21×10^{-10}	2.32	0.616	0.63	0.59	0.59
290	1.69×10^{-9}	2.09	0.668	0.62	0.57	0.58

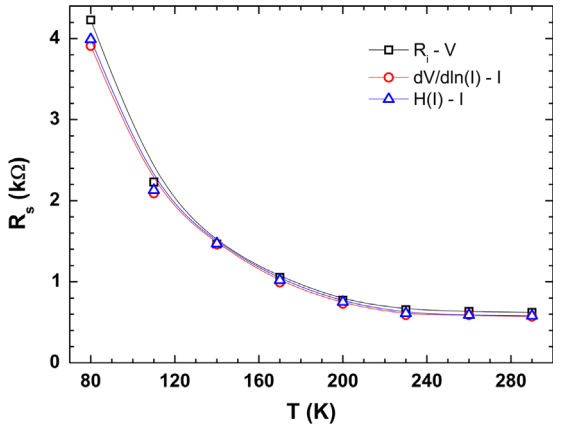

Fig. 3. R_s–T plot of Au/n-Si MS SBD.

$dV/d\ln(I)$ and $H(I)$ vs. I plots of MS SBD were drawn using the following equations and shown in Fig. 2(a) and (b), respectively.

$$dV/d\ln(I) = nkT/q + IR_S \tag{1}$$

$$H(I) = V + (nkT/q)\ln\left[I/AA^*T^2\right] = n\Phi_{Bo} + IR_S \tag{2}$$

Utilizing Eqs. (1) and (2), R_s values were extracted from the slopes of $dV/d\ln(I)$ and $H(I)$ vs. I plots of MS SBD. R_s values obtained via Ohm's law and Cheungs' method are presented in Table 1 along with other electrical parameters that will be obtained in preceding paragraphs. As seen in the table, Cheungs' method reveals R_s values that are quite close those obtained by Ohm's law. R_s values were also plotted against temperature (Fig. 3) in order to interpret temperature dependence. As seen in Fig. 3, R_s values decrease with increasing temperature in consistency with what is observed in other studies in the literature [7,9,12,14].

The linear regions up to 1 V in Fig. 1 are the key to extraction of electrical parameters of MS SBD. For an MS SBD with R_s, the relationship between current and applied bias voltage in terms of TE theory for $V \geq 3kT/q$ is expressed as [2]

$$I = I_o\left[\exp\left(\frac{q(V-IR_s)}{nkT}\right)-1\right] \tag{3}$$

where IR_s is voltage drop caused by R_s of SBD, n is ideality factor, k is Boltzmann constant, T is temperature in Kelvin,

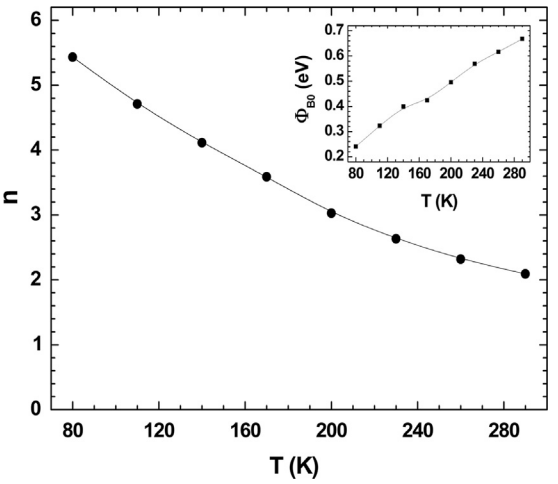

Fig. 4. n–T plots of Au/n-Si MS SBD; inset shows Φ_{Bo}–T plots of Au/n-Si MS SBD.

q is the electronic charge, and I_o is reverse saturation current which is expressed as [2]

$$I_o = AA^*T^2\exp\left(-\frac{q\Phi_{Bo}}{kT}\right) \tag{4}$$

Here A, A^* and Φ_{Bo} are front contact area, effective Richardson constant which is 120 A/cm^2 K^2 for n-Si [2] and the zero-bias barrier height, respectively.

I_o is extracted from the straight-line y-intercept of the current axis in ln$I$–V plots and afterwards Φ_{Bo} can be calculated using Eq. (4). Another important diode parameter n can be obtained from the slope of linear regions in ln$I$–V plots using following equation which is derived from Eq. (3):

$$n = \frac{q}{kT}\frac{dV}{d\ln(I)} \tag{5}$$

Obtained values of I_o, Φ_{Bo} and n are presented in Table 1 for each temperature level and n–T and Φ_{Bo}–T plots are shown in Fig. 4 and its inset, respectively. It is seen that n values are larger than unity. n shows the conformity of MS SBD to TE, i.e. the larger the n, the more the deviation from TE. Hence, obtained n values imply deviation from TE. Particularly at lower temperatures, current flows through the lower patches of barrier potential; therefore this yields larger n values [12–15]; hence this indicates that barrier height might be inhomogeneous. Another reason of such high n values can be attributed to particular distribution of interface traps and their restructuring and reordering under the effect of temperature [17,18]. For this reason D_{it} values of MS SBD were calculated using Chard and Rhoderick's model as in relation below [19]:

$$D_{it} = \frac{1}{q}\left[\frac{\varepsilon_i}{\delta}(n(V)-1)-\frac{\varepsilon_s}{W_D}\right] \tag{6}$$

Here ε_i, δ, ε_s and W_D are permittivity of native insulator layer which is SiO_2 in our case, thickness of interfacial layer, permittivity of semiconductor, and width of space-charge region, respectively. Calculated values D_{it} values of MS SBD were given in D_{it} vs. E_c–E_{ss} plots in Fig. 5 while

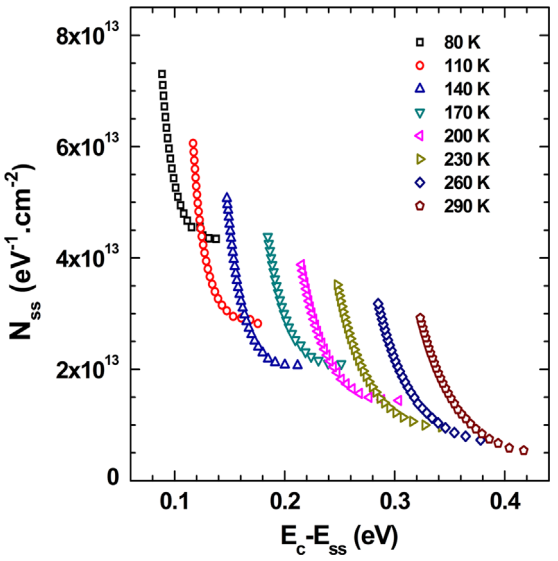

Fig. 5. D_{it} vs. E_c–E_{ss} plots of Au/n-Si MS SBD.

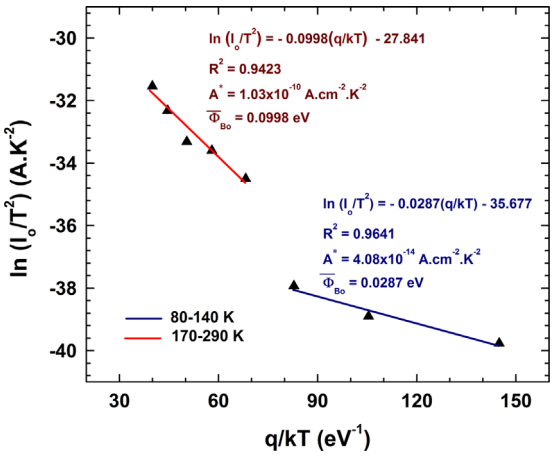

Fig. 6. $\ln(I_o/T^2)$ vs. q/kT plot of Au/n-Si MS SBD.

calculation details of corresponding E_c–E_{ss} values for D_{it} values are given elsewhere [6]. As can be seen in Fig. 5, MS SBD has larger D_{it} values at lower temperatures which explains the higher n values at low temperatures. As the temperature increases, interface traps localize further from lower edge of conduction band of n-Si and at higher temperatures these traps localize in a wider energy gap of E_c–E_{ss}.

As to Φ_{Bo} values, it is seen that Φ_{Bo} increases with increasing temperature on the contrary band gap's behavior with temperature regarding its negative temperature coefficient of -4.73×10^{-4} eV/K. Temperature dependent behavior of n and Φ_{Bo} suggests inhomogeneous barrier height and deviation from the TE theory. In order to check traces of inhomogeneous barrier height, Eq. (4) is rewritten as

$$\ln\left(\frac{I_0}{T^2}\right) = \ln(AA^*) - \frac{q\Phi_{Bo}}{kT} \tag{7}$$

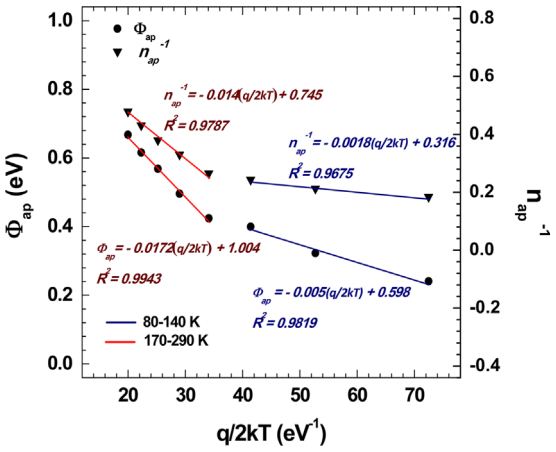

Fig. 7. Φ_{ap} and n_{ap}^{-1} vs. $q/2kT$ plots of Au/n-Si MS SBD.

Using Eq. (7), it is possible to obtain experimental values of A^* and Φ_{Bo} from $\ln(I_o/T^2)$ vs. q/kT plot, which is also called as the Richardson plot. Hence, the Richardson plot of MS SBD is drawn and shown in Fig. 6. As seen in the figure, there are two linear regions whose line equations are also given in the figure. Using these line equations, two different sets of A^* and Φ_{Bo} are obtained as 4.08×10^{-14} A cm^{-2} K^{-2} and 0.0287 eV, and 1.03×10^{-10} A cm^{-2} K^{-2} and 0.0998 eV for 80–140 K and 170–290 K temperature regions, respectively. Indeed, these values of Φ_{Bo} are small and more importantly these values of A^* are much smaller than its reported value. Such small values of A^* and Φ_{Bo} are due to inhomogeneous barrier height which stem from potential fluctuations at the metal–semiconductor interface [10–15,17,18].

In the case of inhomogeneous barrier height, total current passing through the MS SBD is the sum of current for each barrier patch as given below in the integral form [18]

$$I = \int_{-\infty}^{\infty} I(\Phi_B, V)P(\Phi_B)d\Phi \tag{8}$$

where $P(\Phi_B)$ is the probability of accuracy for barrier height which is given by [18]

$$P(\Phi_B) = \frac{1}{\sigma_s\sqrt{2\pi}}\exp\left(-\frac{(\Phi_B-\overline{\Phi}_B)^2}{2\sigma^2}\right) \tag{9}$$

Here $\overline{\Phi}_B$ is mean barrier height and σ_s is standard deviation of barrier height. Solution of the integral in Eq. (8) reveals a current expression as in Eq. (10) which is very similar to the case of TE theory;

$$I = AA^*T^2\exp\left(-\frac{q\Phi_{ap}}{kT}\right)\left[\exp\left(\frac{qV}{n_{ap}kT}\right)-1\right] \tag{10}$$

Φ_{ap} and n_{ap} replaces Φ_{Bo} and n as given below:

$$\Phi_{ap} = \overline{\Phi}_{Bo} - \frac{q}{2kT}\sigma_s^2 \tag{11.a}$$

$$n_{ap}^{-1} = 1 + \rho_2 - \frac{q}{2kT}\rho_3 \tag{11.b}$$

where ρ_2 and ρ_3 are voltage coefficients and they can be obtained from y-intercept and slope values of n_{ap}^{-1} – $q/2kT$ plot, whereas $\overline{\Phi}_{Bo}$and σ_s can be calculated by y-intercept

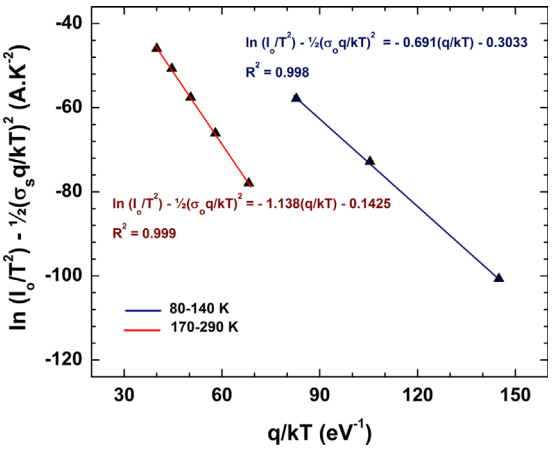

Fig. 8. $\ln(I_0/T^2) - \frac{1}{2}(q\sigma_s/kT)^2$ vs. q/kT plots of Au/n-Si MS SBD.

and slope values of $\Phi_{ap} - q/2kT$ plot. For this purpose, $\Phi_{ap}-q/2kT$ and $n_{ap}^{-1} - q/2kT$ plots of MS SBD and their line equations are depicted in Fig. 7. As seen in Fig. 7, $\overline{\Phi}_{Bo}$ values are 0.598 eV and 1.004 eV for 80–140 K and 170–290 K temperature regions, respectively. Furthermore, using slope values of $\Phi_{ap} - q/2kT$ plots σ_s for 80–140 K and 170–290 K temperature regions were calculated as 0.071 and 0.131, respectively. High σ_s values are another proof that the barrier height is inhomogeneous. At first glance, the difference between σ_s values of each temperature region might seem huge. However the difference between σ_s values can be regarded as reasonable when σ_s is compared with its corresponding $\overline{\Phi}_{Bo}$value.

In order to cross-check obtained σ_s and $\overline{\Phi}_{Bo}$values, modified Richardson plots are depicted in Fig. 8 by combining Eqs. (7) and 11.a into the relation below:

$$\ln\left(\frac{I_0}{T^2}\right) - \frac{1}{2}\left(\frac{q\sigma_s}{kT}\right)^2 = \ln(AA^*) - \frac{q}{kT}\overline{\Phi}_{B0} \tag{12}$$

Experimental values of A^* and Φ_{Bo} were extracted from the line equations given in $\ln(I_0/T^2) - \frac{1}{2}(q\sigma_s/kT)^2$ vs. q/kT plots of MS SBD in Fig. 7. Obtained $\overline{\Phi}_{Bo}$values of 0.691 eV and 1.138 eV for 80–140 K and 170–290 K temperature regions, respectively, are close to those obtained from $\Phi_{ap}-q/2kT$ plots. Moreover, using the y-intercept of modified Richardson plots, A^* values were calculated as 94.1 A cm^{-2} K^{-2} and 110.5 A cm^{-2} K^{-2} for 80–140 K and 170–290 K temperature regions, respectively. These fair values of $\overline{\Phi}_{Bo}$ and A^* confirms that I–V characteristics of Au/n-Si MS SBD can be explained with TE theory with GD of inhomogeneous barrier height.

4. Conclusion

Fabricated Au/n-Si MS SBD's I–V characteristics were investigated in a wide temperature range of 80–290 K. As expected, calculated R_s values decreased with increasing temperature. Using TE theory for MS SBDs with R_s, values of Φ_{Bo} and n are calculated for each temperature level. D_{it} values of MS SBD were calculated; the rise in D_{it} with decreasing temperature was found responsible for higher n values at lower temperatures. Besides the behavior of n with temperature, the rise in Φ_{Bo} with increasing temperature indicated inhomogeneous barrier height. Richardson plots of MS SBD confirmed inhomogeneity in barrier potential; therefore it was concluded that I–V characteristics of MS SBD are governed by TE theory with GD of inhomogeneous barrier height. Obtained reasonable values of $\overline{\Phi}_{Bo}$ and A^* confirmed our conclusion.

References

[1] F. Braun, Ann. Phys. Chem. 153 (1874) 556.
[2] S.M. Sze, Physics of Semiconductor Device, 2nd ed, Wiley, New York, 1981.
[3] M. Yıldırım, P. Durmuş, Ş. Altındal, Chin. Phys. B 22 (2013) 108502.
[4] P. Durmuş, M. Yıldırım, Ş. Altındal, Curr. Appl. Phys. 13 (2013) 1630.
[5] M. Yıldırım, M. Gökçen, Mater. Sci. Semicond. Process. 15 (2012) 406.
[6] H. Uslu, M. Yıldırım, Ş. Altındal, P. Durmuş, Radiat. Phys. Chem. 81 (2012) 362.
[7] A. Hussain, A. Rahman, Mater. Sci. Semicond. Process. 16 (2013) 1918.
[8] H. Kim, H. Kim, D.-W. Kim, J. Korean Phys. Soc. 63 (2013) 2034.
[9] I. Jyothi, M.-W. Seo, V. Janardhanam, K.-H. Shim, Y.-B. Lee, K.-S. Ahn, C.-J. Choi, J. Alloys Compd. 556 (2013) 252.
[10] S. Chirakkara, S.B. Krupanidhi, Thin Solid Films 520 (2012) 5894.
[11] A. Chawanda, W. Mtangi, F.D. Auret, J. Nel, C. Nyamhere, M. Diale, Physica B 407 (2012) 1574.
[12] K.R. Peta, B.-G. Park, S.-T. Lee, M.-D. Kim, J.-E. Oh, Microelectron. Eng. 93 (2012) 100.
[13] E. Özavcı, S. Demirezen, U. Aydemir, Ş. Altındal, Sens. Actuator A: Phys. 194 (2013) 259.
[14] W.-C. Huang, T.-C. Lin, C.-T. Horng, Y.-H. Li, Mater. Sci. Semicond. Process. 16 (2013) 418.
[15] M. Gökçen, M. Yıldırım, Chin. Phys. B 21 (2012) 128502.
[16] D.E. Yildiz, D.H. Apaydin, E. Kaya, S. Altindal, A. Cirpan, J. Macromol. Sci. A 50 (2013) 168.
[17] P. Chattopadhyay, A.N. Daw, Solid-State Electron. 29 (1986) 555.
[18] J.H. Werner, H.H. Guttler, J. Appl. Phys. 69 (1991) 1522.
[19] C. Card, E.H. Rhoderick, J. Phys. D: Appl. Phys. 4 (1971) 1589.